Available online at www.sciencedirect.com
ScienceDirect
Ceramics International 37 (2011) 1109–1113
CERAMICS INTERNATIONAL
www.elsevier.com/locate/ceramint

Short communication

Increases in the strength of Si-additive mixture granules by presintering

Young-Jo Park *, Boo-Won Park, Jae-Wook Lee, Hui-Suk Yun, In-Hyuck Song

Engineering Ceramics Research Group, Korea Institute of Materials Science, 797 Changwondaero, Changwon, Gyeongnam 641-831, Republic of Korea

Received 23 July 2010; received in revised form 23 August 2010; accepted 6 October 2010
Available online 17 November 2010

Abstract

In order to preserve a spherical granule shape in a porous sintered body, presintering technology was developed to enhance the strength of Si-mixture granules containing Y_2O_3–Al_2O_3–CaO as sintering additives prior to shaping. The fracture strength of the granules measured by a compression test was ≤0.2 MPa and ≤20 MPa for as-spray dried granule and presintered granules, respectively. Furthermore, the flowability of the presintered granules was retained by the presintering process done to 1300 °C.

Keywords: D. Nitrides; Granular materials; Porous

1. Introduction

The morphology of silicon nitride (Si_3N_4) ceramics which consists of a rod-like grain makes these materials excellent for use in filtering media due to their complex pore-channel path and large specific surface area [1–3]. However, the diameter (ϕ) of the pore channels in porous SRBSNs (sintered reaction-bonded silicon nitrides) is usually restricted to ~1 μm due to: (1) the nitriding mechanism, which involves both gas and solid phases; and (2) the limitation of the grain size (d) by the liquid phase sintering vehicle (d = 1–2 μm) [3–5]. Because a large pressure drop develops across current SRBSN filter materials with narrow pore channels, the widening of pore channels to match the size of commercially available filters (ϕ > 10 μm) is strongly desired. In this research, simultaneous enhancement of both filtering efficiency and permeability of SRBSN filter was pursued through the granulation of the starting powders. In this approach, wide channels (≥10 μm), for permeability, form between the granules while narrow channels (<0.5 μm), for trapping particles, form inside the granules. However, it is difficult to preserve the spherical morphology of the granules by conventional shaping methods due to the fragile characteristics of the as-spray dried granule (as-SD) [6,7]. Here, we report that granule strength can be enhanced by a presintering treatment done above the eutectic point of the sintering additive system. For the additives used in this study (Y_2O_3–Al_2O_3–CaO_2), the lowest eutectic temperature was 1170 °C resulting in an Al_2O_3–CaO–SiO_2 ternary system. Since the form of SiO_2 exists as a native oxide layer on Si powders, the presintering temperature as a result can be set between 1170 °C and 1412 °C (the melting point of Si). Here, the presintering processing window that achieves intragranular bonding without intergranular bonding was investigated. Such bonding permits an increase in granule strength of the presintered granules (PGs) without a loss of flowability of the as-spray dried granule (as-SD).

2. Experiment

The commercially available silicon powder used in this study had a purity greater than 98.6% (Sicomill grade 2, Vesta Ceramics, Ljungaverk, Sweden; 0.4 wt% Fe, 0.2 wt% Al, 0.2–1.0 wt% O, d_{50} = 2 μm). The following commonly adopted oxide sintering additives were used: Y_2O_3 (Grade C, H.C. Stark, Goslar, Germany; 99.99%, d_{50} = 0.7 μm), Al_2O_3 (AKP-30, Sumitomo, Tokyo, Japan; 99.99%, d_{50} = 0.31 μm), and $CaCO_3$ (Sigma–Aldrich, 99+% purity) as the source of CaO. The total amount of sintering additives (3 wt%) was based on the Si_3N_4 content calculated from the perfect nitridation of Si. Polyacrylic acid (PAA; Wako, Tokyo, Japan) and polyvinyl alcohol (PVA; Junsei, Tokyo, Japan) were blended in the Si-additive mixture as dispersant and binder, respectively. The amount of PAA and PVA were 0.5 wt% and 2 wt%,

* Corresponding author at: 737 Changwondaero, Changwon, Gyeongnam 641-831, Republic of Korea. Tel.: +82 55 280 3356; fax: +82 55 280 3392.
E-mail address: yjpark87@kims.re.kr (Y.-J. Park).

0272-8842/$36.00
doi:10.1016/j.ceramint.2010.10.013

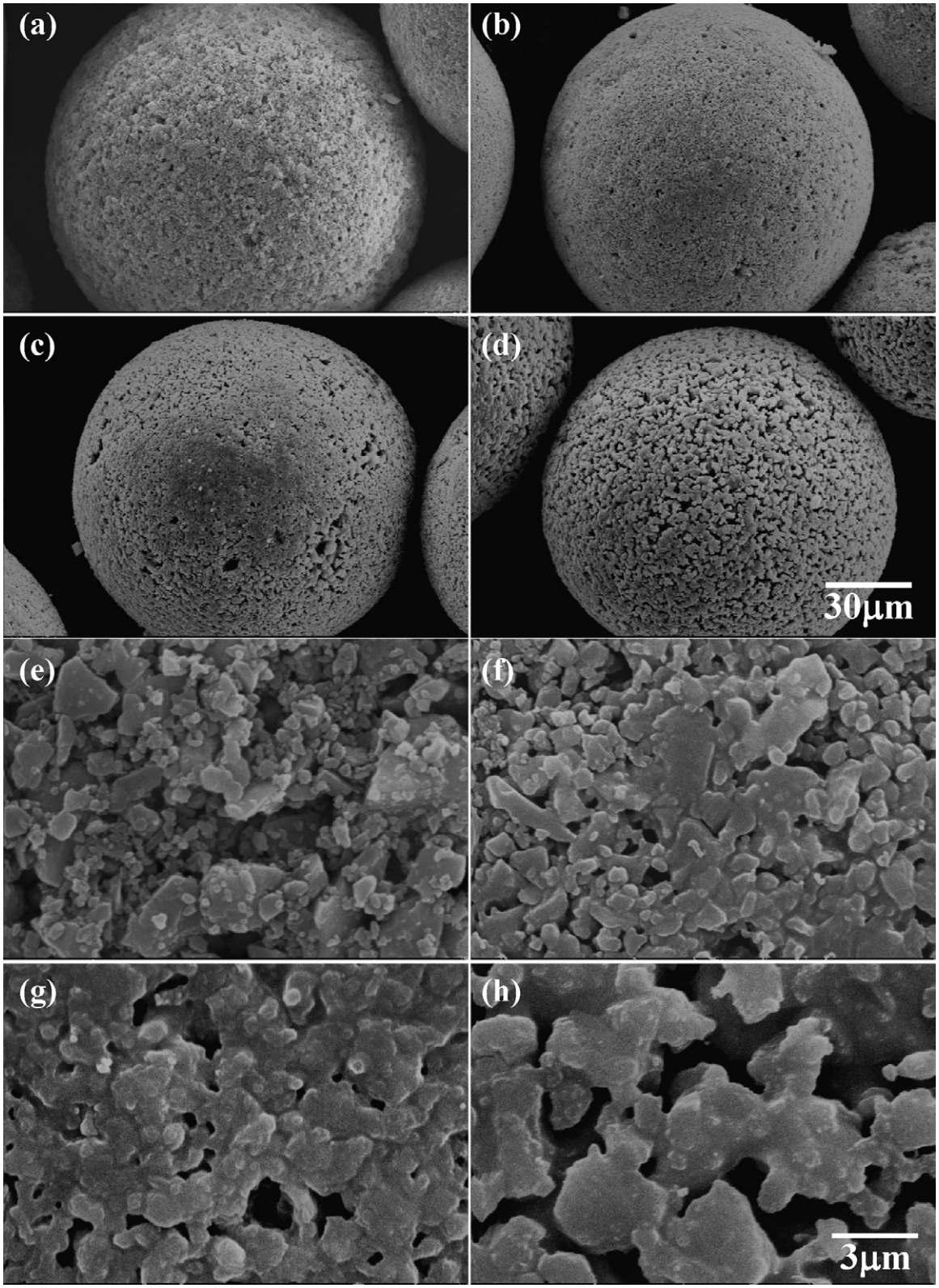

Fig. 1. Morphology of the granule surfaces of as-SD and PGs. (a and e) as-SD, (b and f) PG1 (1200 °C, 10 min), (c and g) PG3 (1300 °C, 10 min), and (d and h) PG4 (1350 °C, 10 min). (a)–(d) Low magnification (1k×) and (e)–(h) high magnification (10k×).

respectively, of the sum of the other solid ingredients (Table 1). Prior to spray drying, the obtained slurry was mixed by planetary milling for 2 h using an equal weight of water and Si-additive mixture (Table 1). Granules were fabricated by spray drying using an atomizer speed of 10,000 r/min with inlet and outlet temperatures fixed at 250 °C and 110 °C, respectively. The size of the granules ranged from 30 μm to 150 μm. The presintering of the granules was done using a tube furnace

Table 1
Composition of the Si-additive slurry used for spray drying.

Si (g)	Y_2O_3 (g)	Al_2O_3 (g)	$CaCO_3$ (g)	PAA (g)	PVA (g)	Water (g)
100	2.67	1.33	2.05	0.53	2.12	108.7

soaking at 1200–1350 °C for 10 min under a flowing (150 ml/min) Ar atmosphere. An additional prolonged presintering time of 60 min was done at 1200 °C. The flowability of the granules before and after presintering was evaluated by measuring the passing time of 5 g of dried granules through an orifice with a diameter of 2.54 cm. The compacting behavior of the granules, e.g., density *vs.* compacting pressure, was derived from the obtained load *vs*. displacement relationship in a displacement-controlled compression test (0.5 mm/min) using a 10 mm diameter cylindrical mold. The weight of the granules for the compression charge was 0.8 g. A scanning electron microscope (SEM; JSM-6700F, JEOL, Tokyo, Japan) was used to observe the microstructures. X-ray diffraction (XRD; D/Max 2200, Rigaku, Tokyo, Japan) was done for phase identification.

3. Results and discussion

Fig. 1 shows the comparison of the granule surfaces before (a and e) and after (b, c, d, f, g, and h) presintering treatment. It is evident, at low magnification, that the surface roughness has decreased in PG1 (Fig. 1(b)) compared to as-SD (Fig. 1(a)). On the other hand, the surfaces of PG3 (Fig. 1(c)) and PG4 (Fig. 1(d)) have a more roughened surface. High magnification clearly shows that individual starting particles in as-SD (Fig. 1(e)) are penetrated by amorphous phases in the PGs (Fig. 1(f–h)). That is, decreased roughness in PG1 is attributed to the filling of pits at the surface by glass phases while the increases in surface roughness for PG3 and PG4 was due to the severe agglomeration of particles caused by both the increased amount and decreased viscosity of the liquid phase as presintering temperature reached over 1300 °C.

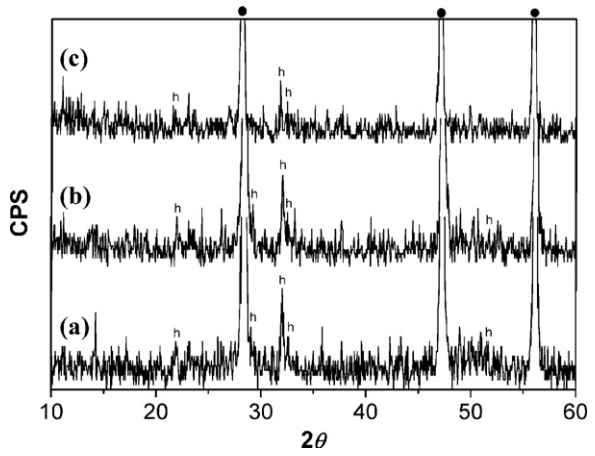

Fig. 2. XRD analysis of presintered granules. (a) PG1 (1200 °C, 10 min), (b) PG3 (1300 °C, 10 min), (d) PG4 (1350 °C, 10 min). In the figure, symbol (●) stands for Si and symbol (h) stands for h-phase ($Y_5Si_3Al_{12}N$).

XRD analysis revealed that oxynitride h-phase ($Y_5Si_3O_{12}N$) formed in all the PGs of the current experiment (Fig. 2). As the tube furnace used for the presintering was not equipped with a vacuum facility, the remnant air in the tube under the flowing Ar reacted as the source of nitrogen for the formation of h-phase. It is well known that the formation of h-phase is facilitated by the solution-precipitation vehicle through the eutectic liquid phase. The other starting components except for Si were not detected since there was only a small amount in the starting materials.

The apparent flowability of the PGs under various heat-treatment conditions (PG1–PG4) appeared to be similar to that of as-SD. Therefore, the measurement of flowability was done only for as-SD, PG1 and PG4. Nearly the same values for flowability (0.4136 g/s for as-SD and 0.4068 g/s for PG1) were obtained indicating that intergranular sintering was avoided under low temperatures (1200 °C) and short condition times (10 min). It is postulated that this result is due to the liquid phase being confined within the granules by capillary forces so that the necks between granules were not wetted. While, decreased flowability in PG4, 0.3180 g/s, was caused by the roughened surfaces as depicted in Fig. 1(d and h) rather than intergranular bonding.

Fig. 3(a) presents the load *vs*. displacement relationship in the compression test for as-SD and PGs. The abrupt increase in load at a specific displacement (Fig. 3(a)) is ascribed to an increase in the packing density (Fig. 3(b)) caused by the facture of granules [8]. The largest displacement shown in as-SD prior to that dramatic increase in load reflects deformation of the granules which is not seen in the PGs. Furthermore, the same analogy may be applied to the earlier steep rise in the stiffer PG3 (presintered at 1300 °C) and PG4 (presintered at 1350 °C) compared to the gentle rise in the less stiff PG1 and PG2 (both presintered at 1200 °C). The prolonged soaking time (60 min, PG2) at 1200 °C only led to a slight change in the granule strength compared to the 10 min soaking time (PG1). The fact that there is a greater dependency on temperature rather than sintering time for granule strength supports the hypothesis from the current research that strengthening of the granules relies on the degree of liquid phase sintering. The compacting behaviors of as-SD and PGs are plotted in Fig. 3(b). The relationship of the density *vs.* the compacting pressure was derived from the geometry of the mold and the mass of the granules combined with load *vs*. displacement data summarized in Fig. 3(a). In the figure, the compacting pressure at the inflection point represents the fracture strength of the granules beyond which the green body undergoes substantial densification [8]. The fracture strengths were $\leq$0.2 MPa, $\leq$5 MPa, $\leq$10 MPa and $\leq$20 MPa for as-SD, PG1/PG2, PG3, and PG4, respectively. Depending on the presintering conditions, approximately 25–100-fold increases in granule strength were achieved. In

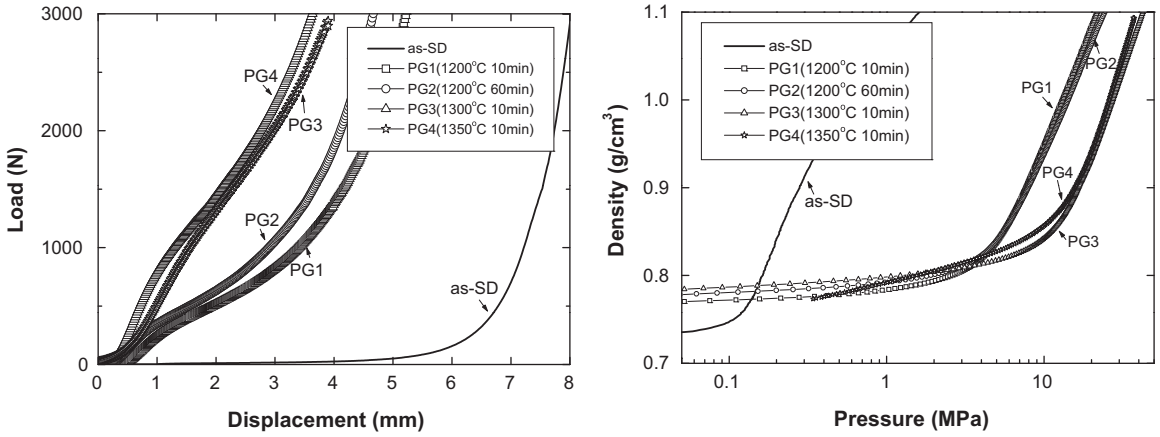

Fig. 3. Load (N)–displacement (mm) relationship (a) and density (g/cm^3)–compacting pressure (MPa) relationship (b) acquired from compression test on as-SD and PGs.

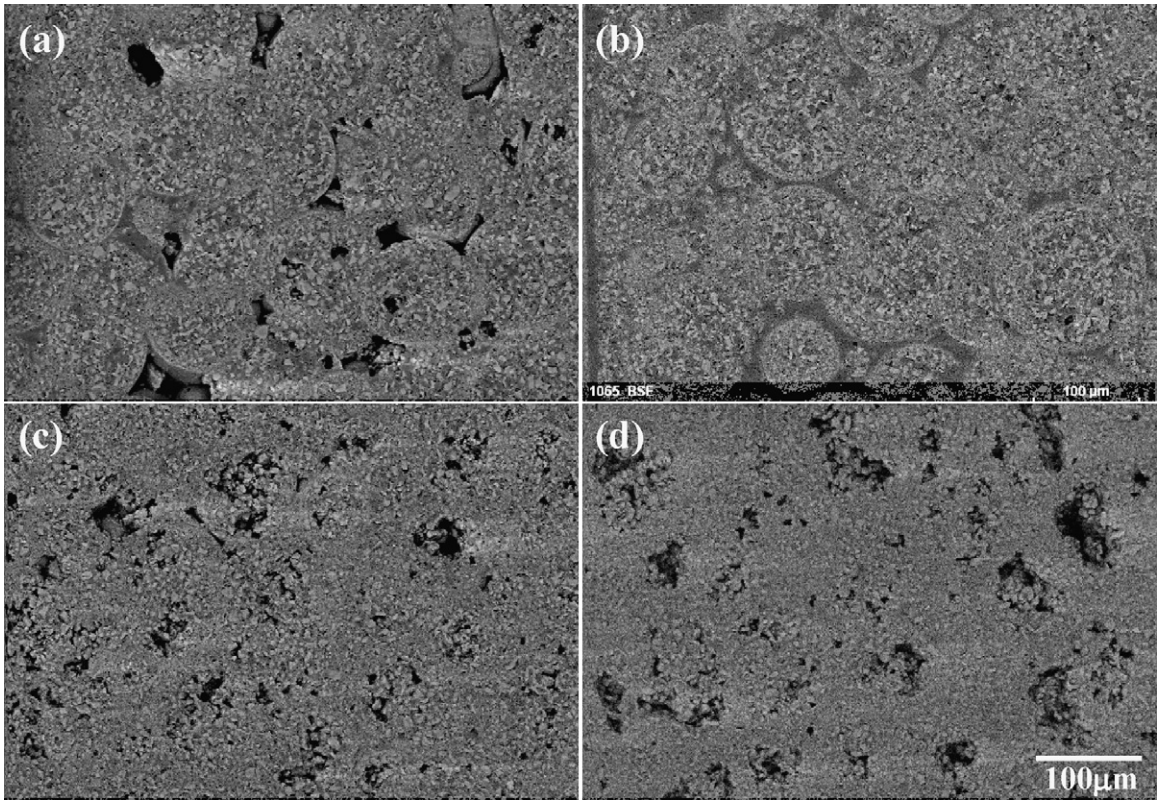

Fig. 4. SEM micrographs of the polished surfaces of uniaxially pressed PG1 (presintered at 1200 °C for 10 min). Specimens are pressed at (a) 3.7 MPa, (b) 7.5 MPa, (c) 18.6 MPa, and (d) 46.6 MPa.

addition, Fig. 3(b) shows that the initial density of as-SD is lower than those of PGs; however, above ∼0.15 MPa of the compacting pressure, the density of as-SD was always higher than those of PGs. We suggest that this is related to the accelerated packing of the easily fractured as-spray dried fragile granules.

SEM micrographs of the polished surfaces of uniaxially pressed PG1 (1200 °C, 10 min) are shown in Fig. 4. Four pressing levels from 3.7 MPa to 46.6 MPa were tested after taking into consideration the ∼5 MPa granule strength of PG1 (see Fig. 3(b)). The spherical morphology of the presintered granules was preserved up to a pressing pressure of 7.5 MPa (Fig. 4(a and b)) while fracturing of the granules occurred by pressing at 18.6 MPa and 46.6 MPa (Fig. 4(c and d)). We infer from these microstructures that continuous pore channels between granules can be formed by pressing PGs below the granule strength because of the retention of non-fractured spherical granules. In those low pressure images, some open channels are visible while others are filled with mounting resins used for the polishing (Fig. 4(a and b)). In contrast, as a consequence of the deforming of granule spheres followed by fracturing, only isolated pore pockets are visible in the higher pressure images (Fig. 4(c and d)).

4. Conclusions

In order to take advantage of the rod-like grain morphology of porous SRBSNs, it is crucial to preserve the spherical shape of granules for the formation of wide channels to meet the requirement of permeability. Here, a presintering technique was developed for granules of Si powders mixed with Y_2O_3–Al_2O_3–CaO additives. Heat treatment between 1200 °C and 1300 °C resulted in nearly the same level of flowability as that of as-SD with enhanced granule strength. The fracture strength of the granules measured by compression test ranged from $\leq$0.2 MPa to $\leq$20 MPa for as-SD and PGs, respectively. Considering the shaping pressures tested in this study, the implications for these strengthened granules for industrial application are promising.

Acknowledgement

This research project was supported by the Korea Institute of Materials Science, a branch of Korea Institute of Machinery and Materials.

References

[1] K. Kawai, A. Yamakawa, Effect of porosity and microstructure on the strength of Si_3N_4: designed microstructure for high strength, high thermal shock resistance, and facile machining, J. Am. Ceram. Soc. 80 (1997) 2705–2708.
[2] N. Miyakawa, H. Sato, H. Maeno, H. Takahashi, Characteristics of reaction-bonded porous silicon nitride honeycomb for DPF substrate, JSAE Rev. 24 (2003) 269–276.
[3] Y.J. Park, E. Choi, H.W. Lim, H.D. Kim, Design of porosity level for porous Si_3N_4 ceramics manufactured by nitriding and post-sintering of Si powder compact, Mater. Sci. Forum 534–536 (2007) 1017–1020.
[4] D.S. Park, M.W. Lee, Y.J. Park, H.D. Kim, Y.G. Jung, Fabrication and properties of porous RBSN, Key Eng. Mater. 287 (2005) 277–281.
[5] D.V. Tuyen, Y.J. Park, H.D. Kim, B.T. Lee, Formation of rod-like Si_3N_4 grains in porous SRBSN bodies using $6Y_2O_3$–2MgO sintering additives, Ceram. Int. 35 (2009) 2305–2310.
[6] D.C.C. Lam, Effects of binder and compaction pressure on strength and fracture origins in bodies pressed from granules, J. Ceram. Soc. Jpn. 102 (1994) 1010–1015.
[7] E. Horisawa, A. Komura, K. Danjo, A. Otsuka, Effect of granule strength on compressed tablet strength, Chem. Pharm. Bull. 43 (1995) 2261–2263.
[8] Y. Kondo, Y. Hashizuka, M. Nakahara, K. Yokota, Granule properties in uniaxial press forming of alumina ceramics, J. Ceram. Soc. Jpn. 103 (1995) 1037–1040.